2016 IEEE 55th Conference on Decision and Control (CDC)
ARIA Resort & Casino
December 12-14, 2016, Las Vegas, USA

Adaptive Input Estimation for Nonminimum-Phase Discrete-Time Systems

Ahmad Ansari and Dennis S. Bernstein

Abstract— **The accuracy of state estimation can be enhanced by simultaneously estimating unknown inputs. This paper presents an extension of retrospective cost input estimation (RCIE) that directly updates the estimates of all states. We show that RCIE can be used for systems in which the transmission zeros from the estimated input to the measurement are nonminimum phase. We demonstrate this ability on numerical examples, and we compare the estimates from RCIE to estimates from prior methods for input estimation. Finally, we use this technique to estimate the acceleration of a flight vehicle using camera data, and we assess the accuracy of the acceleration estimates by transforming the onboard body-frame acceleration measurements to the camera frame.**

I. Introduction

The goal of classical state estimation is to use the dynamics model in conjunction with state measurements to estimate unmeasured states and filter the noise corrupting the measurements. The process noise w is modeled as a zero-mean white random process whose statistical properties are known. If an additional known input u drives the system, then u can be replicated in the estimator dynamics in order to reduce the state-estimation error. The input u may be either a deterministic or random signal.

In many practical situations, it may be desirable to estimate the exogenous input, or at least a portion of it. In particular, the exogenous input may consist of a combination of random process noise w, a known input u, and an unknown deterministic or random input d. The distinction between w and d is the desire to estimate d in order to replicate it in the estimator and thereby reduce the error in the state estimates.

The literature on input estimation is extensive, and various techniques have been proposed [1]–[10]. In [11], [12], the more limited goal is to obtain unbiased state estimates without obtaining an estimate of the unknown input d. The present paper addresses the input estimation problem based on retrospective cost optimization [13]–[17]. Retrospective cost input estimation was demonstrated in [13] and applied in [14]–[17] to atmospheric estimation, acceleration estimation, and fault diagnosis.

The goal of the present paper is to extend the approach used in [14]–[16] by modifying the adaptive input estimation subsystem so that it directly updates the estimates of all states as in the case of the Kalman filter data injection term $K(y - C\hat{x})$. We then compare this retrospective cost input estimation (RCIE) technique to the input reconstruction methods in [1] and [10]. In particular, the filters in [1] and [10] are confined to systems in which the dynamics from the estimated unknown input to the measurement are minimum phase. In contrast, the approach of the present paper applies to the case where these dynamics have nonminimum-phase transmission zeros. This feature is demonstrated for a collection of numerical examples. We also apply RCIE to laboratory data, where the goal is to estimate the acceleration of a flight vehicle using vision data. The accuracy of RCIE is assessed by comparing the acceleration estimates to the acceleration measurements provided by the on-board accelerometers transformed to the camera frame.

Ahmad Ansari, and Dennis S. Bernstein are with the Department of Aerospace Engineering, University of Michigan, Ann Arbor, MI, USA. {ansahmad, dsbaero}@umich.edu

II. Problem Formulation

Consider the linear time-invariant system

$$x(k)=Ax(k-1)+Bu(k-1)+Gd(k-1)+D_1w(k-1), \quad (1)$$

$$y(k)= Cx(k) + D_2v(k), \quad (2)$$

where $x(k) \in \mathbb{R}^{l_x}$ is the unknown state, $u(k) \in \mathbb{R}^{l_u}$ is the known input, $d(k) \in \mathbb{R}^{l_d}$ is the unknown input, $D_1w(k) \in \mathbb{R}^{l_x}$ is the process noise with known covariance $V_1 \stackrel{\triangle}{=} D_1D_1^{\mathrm{T}} \in \mathbb{R}^{l_x\times l_x}$, $y(k) \in \mathbb{R}^{l_y}$ is the measured output, and $D_2v(k) \in \mathbb{R}^{l_v}$ is the measurement noise with known covariance $V_2 \stackrel{\triangle}{=} D_2D_2^{\mathrm{T}} \in \mathbb{R}^{l_y\times l_y}$. The matrices $A \in \mathbb{R}^{l_x\times l_x}$, $B \in \mathbb{R}^{l_x\times l_u}$, $G \in \mathbb{R}^{l_x\times l_d}$, and $C \in \mathbb{R}^{l_y\times l_x}$ are assumed to be known. The goal is to estimate the unknown input $d(k)$ and the unknown state $x(k)$. The system (1), (2) is minimum phase (MP) if the transmission zeros of (A, G, C) are contained in the open unit disk; otherwise (1), (2) is nonminimum phase (NMP).

At each time step k, we estimate the unknown input $d(k-1)$ and the unknown state $x(k)$ using the measured output $y(k)$ in the following two steps:

1. In the input estimation step, we estimate $d(k-1)$ using the estimate of $x(k-1)$.
2. In the state estimation step, we estimate $x(k)$ using the estimate of $d(k-1)$.

A. Retrospective Cost Input Estimation (RCIE)

In order to estimate the unknown input $d(k-1)$, we consider the update equations

$$\hat{x}(k) = Ax_{\mathrm{da}}(k-1) + Bu(k-1) + G\hat{d}(k-2), \quad (3)$$

$$\hat{y}(k) = C\hat{x}(k), \quad (4)$$

$$z(k) = \hat{y}(k) - y(k), \quad (5)$$

where $\hat{x}(k) \in \mathbb{R}^{l_x}$ is the forecast state, $\hat{d}(k) \in \mathbb{R}^{l_d}$ is the input estimate, $x_{\mathrm{da}}(k) \in \mathbb{R}^{l_x}$ is the state estimate, and $z(k) \in \mathbb{R}^{l_y}$ is the output error. As shown below, $\hat{d}(k-1)$ is estimated

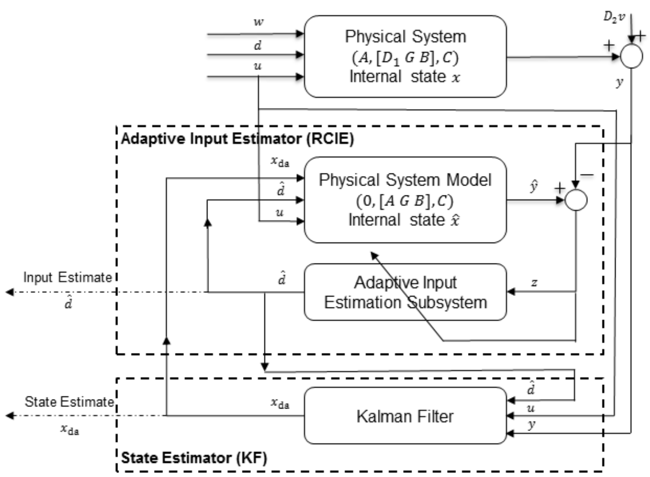

Fig. 1: Input and state estimation architecture. RCIE uses z to update the adaptive input estimation subsystem with input z in order to generate the input estimate $\hat{d}$ that minimizes z. The Kalman filter uses the estimated input $\hat{d}$ in place of d to estimate the unknown state x of the physical system.

at time step k, and thus we use $\hat{d}(k-2)$ estimated at time step $k-1$, in (3) to compute the output error $z(k)$. The goal is to develop an adaptive input estimator that minimizes $z(k)$ by estimating $d(k-1)$.

We obtain the input estimate $\hat{d}(k-1)$ as the output of the *adaptive input-estimation subsystem* of order $n_{\rm c}$ given by

$$\hat{d}(k-1) = \sum_{i=2}^{n_{\rm c}+1} P_i(k)\hat{d}(k-i) + \sum_{i=k_0}^{n_{\rm c}} Q_i(k)\xi(k-i), \quad (6)$$

where $P_i(k) \in \mathbb{R}^{l_d \times l_d}$, $Q_i(k) \in \mathbb{R}^{l_d \times l_\xi}$, $k_0 \geq 0$, and $\xi(k) \in \mathbb{R}^{l_\xi}$ consists of components of y and z. RCIE minimizes $z(k)$ by updating $P_i(k)$ and $Q_i(k)$. Fig. 1 shows the structure of (1)–(6). The subsystem in (6) can be reformulated as

$$\hat{d}(k-1) = \Phi(k)\theta(k), \quad (7)$$

where the regressor matrix $\Phi(k)$ is defined by

$$\Phi(k) \triangleq \begin{bmatrix} \hat{d}(k-2) \\ \vdots \\ \hat{d}(k-n_{\rm c}-1) \\ \xi(k-k_0) \\ \vdots \\ \xi(k-n_{\rm c}) \end{bmatrix}^{\rm T} \otimes I_{l_d} \in \mathbb{R}^{l_d \times l_\theta}$$

and

$$\theta(k) \triangleq \mathrm{vec}\left[\ P_2(k) \cdots P_{n_{\rm c}+1}(k)\ Q_{k_0}(k) \cdots Q_{n_{\rm c}}(k)\ \right] \in \mathbb{R}^{l_\theta},$$

where $l_\theta \triangleq l_d^2 n_{\rm c} + l_d l_\xi (n_{\rm c} + 1 - k_0)$, "$\otimes$" is the Kronecker product, and "vec" is the column-stacking operator.

1) Retrospective Performance: Define $G_{\rm f}({\rm q}) \triangleq D_{\rm f}^{-1}({\rm q})N_{\rm f}({\rm q})$, where q is the forward shift operator, $n_{\rm f} \geq 1$ is the order of $G_{\rm f}$ and

$$N_{\rm f}({\rm q}) \triangleq K_1 {\rm q}^{n_{\rm f}-1} + K_2 {\rm q}^{n_{\rm f}-2} + \cdots + K_{n_{\rm f}}, \quad (8)$$

$$D_{\rm f}({\rm q}) \triangleq I_{l_y} {\rm q}^{n_{\rm f}} + A_1 {\rm q}^{n_{\rm f}-1} + A_2 {\rm q}^{n_{\rm f}-2} + \cdots + A_{n_{\rm f}}. \quad (9)$$

Furthermore, $K_i \in \mathbb{R}^{l_y \times l_d}$ for $1 \leq i \leq r$, $A_j \in \mathbb{R}^{l_y \times l_y}$ for $1 \leq j \leq r$, and $\det(D_{\rm f}({\rm q}))$ is asymptotically stable. Next, for $k \geq k_0$, we define the retrospective performance variable

$$\hat{z}(\hat{\theta}, k) \triangleq z(k) + \Phi_{\rm f}(k)\hat{\theta} - \hat{d}_{\rm f}(k-1), \quad (10)$$

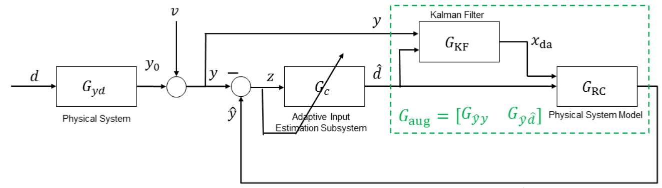

Fig. 2: Input estimation as a control problem. The output $\hat{d}$ of the adaptive input estimation subsystem $G_{\rm c}$ is one of the two inputs of the linear system $G_{\rm aug}$ with output $\hat{y}$. Thus the goal of estimating the unknown input d is equivalent to controlling $G_{\rm aug}$ using its input $\hat{d}$ so that $\hat{y}$ follows the output measurement y. Consequently, $\hat{d}$ follows d.

where

$$\Phi_{\rm f}(k) \triangleq G_{\rm f}({\rm q})\Phi(k), \quad \hat{d}_{\rm f}(k-1) \triangleq G_{\rm f}({\rm q})\hat{d}(k-1), \quad (11)$$

and $\hat{\theta} \in \mathbb{R}^{l_\theta}$ is determined by optimization below.

2) Markov Parameters: To construct the filter $G_{\rm f}$, we consider input estimation as a control problem, as shown in Figure 2. The physical system G_{yd}, physical system model $G_{\rm RC}$ and adaptive input-estimation subsystem G_c in Figure 2 represent (1)–(2), (3)–(4) and (6), respectively. For simplicity, the known input u and the process noise w is not shown. The output $\hat{d}$ of G_c is one of the two inputs of the linear system $G_{\rm aug}$ with output $\hat{y}$. The other input of $G_{\rm aug}$ is the measured output y of G_{yd}. The output $\hat{y}$ is given by

$$\hat{y} = G_{\hat{y}y} y + G_{\hat{y}\hat{d}}\hat{d}, \quad (12)$$

where the $G_{\hat{y}y}$ and $G_{\hat{y}\hat{d}}$ are the components of the transfer matrix $G_{\rm aug}$ given by

$$G_{\rm aug} = \begin{bmatrix} G_{\hat{y}y} & G_{\hat{y}\hat{d}} \end{bmatrix}. \quad (13)$$

Thus the goal of estimating the unknown input d is equivalent to controlling $G_{\rm aug}$ using its input $\hat{d}$ so that $\hat{y}$ follows the output measurement y. Consequently, $\hat{d}$ follows d.

For simplicity, we omit the known input u in (3) and write the physical system model $G_{\rm RC}$ as

$$\hat{x}(k) = A x_{\rm da}(k-1) + G\hat{d}(k-2). \quad (14)$$

We define $x_{\rm d}(k) \triangleq \hat{d}(k-1)$ and rewrite (14) as

$$\begin{bmatrix} \hat{x}(k) \\ x_{\rm d}(k) \end{bmatrix} = \begin{bmatrix} 0 & G \\ 0 & 0 \end{bmatrix} \begin{bmatrix} \hat{x}(k-1) \\ x_{\rm d}(k-1) \end{bmatrix} + \begin{bmatrix} A \\ 0 \end{bmatrix} x_{\rm da}(k-1) + \begin{bmatrix} 0 \\ I \end{bmatrix} \hat{d}(k-1). \quad (15)$$

The closed-loop form of the Kalman filter is given as

$$x_{\rm da}(k) = (A - K_{\rm da}(k-1)CA)\, x_{\rm da}(k-1) + (G - K_{\rm da}(k-1)CG)\hat{d}(k-1) + K_{\rm da}(k-1)y(k), \quad (16)$$

where $K_{\rm da}$ is defined by (27). Using (15) and (16), the state space realization of the linear system $G_{\hat{y}\hat{d}}$ in (13) is as

$$\bar{x}(k) = \bar{A}(k-1)\bar{x}(k-1) + \bar{G}(k-1)\hat{d}(k-1), \quad (17)$$

$$\hat{y} = \bar{C}(k)\bar{x}(k), \quad (18)$$

where

$$\bar{x}(k) \triangleq \begin{bmatrix} \hat{x}(k) \\ x_{\rm d}(k) \\ x_{\rm da}(k) \end{bmatrix}, \bar{A}(k) \triangleq \begin{bmatrix} 0 & G & A \\ 0 & 0 & 0 \\ 0 & 0 & A - K_{\rm da}(k)CA \end{bmatrix}, \quad (19)$$

$$\bar{G}(k) \triangleq \begin{bmatrix} 0 \\ I \\ G - K_{\rm da}(k)CG \end{bmatrix}, \bar{C}(k) \triangleq \begin{bmatrix} C & 0 & 0 \end{bmatrix}. \quad (20)$$

The filter $G_{\rm f}$ at time step k is based on the Markov parameters of the estimated-input-to-estimated-output transfer matrix $G_{\hat{y}\hat{d}}({\rm q},k) = \bar{C}(k)({\rm q}I - \bar{A}(k{-}1))^{-1}\bar{G}(k{-}1)$. For each complex number z whose absolute value is greater than the spectral radius of $\bar{A}$, it follows that

$$G_{\hat{y}\hat{d}}({\rm z},k) = \sum_{i=0}^{\infty} \frac{1}{{\rm z}^i} H_i(k), \tag{21}$$

where, for all, $i \geq 1$, the $i^{\rm th}$ Markov parameter of $G_{\hat{y}\hat{d}}({\rm z},k)$ is defined by

$$H_i(k) \triangleq \begin{cases} 0, & i{=}0 \\ \bar{C}(k{+}i)\bar{G}(k), & i{=}1 \\ \bar{C}(k{+}i)\left(\prod_{j=1}^{j=i-1}\bar{A}(k{+}j)\right)\bar{G}(k), & i{\geq}2. \end{cases} \tag{22}$$

By truncating (21) at each time step k, $G_{\rm f}$ is chosen to be the time-varying Markov-parameter-based finite-impulse-response (FIR) filter

$$G_{\rm f}({\rm q},k) = \sum_{i=0}^{n_{\rm f}} \frac{1}{{\rm q}^i} H_i(k - n_{\rm f}). \tag{23}$$

The order $n_{\rm f}$ is chosen to be sufficiently large that $G_{\rm f}$ approximates the NMP zeros of $(\bar{A}, \bar{G}, \bar{C})$.

3) Cumulative Cost and RCIE Update: For $k > k_0$, we define the cumulative cost function

$$J(k,\hat{\theta}) \triangleq \sum_{i=k_0}^{k} \left(\hat{z}(\hat{\theta},i)^{\rm T} R_z \hat{z}(\hat{\theta},i) + [\Phi(i)\hat{\theta}]^{\rm T} R_d \Phi(i)\hat{\theta}\right) + [\hat{\theta} - \theta(0)]^{\rm T} R_\theta [\hat{\theta} - \theta(0)], \tag{24}$$

where R_z and R_θ are positive definite, and R_d is positive semi-definite. Let $P(0) = R_\theta^{-1}$ and $\theta(0) = \theta_0$. Then, for all $k \geq k_0$, the cumulative cost function (24) has the unique global minimizer $\hat{\theta} = \theta(k)$ given by the RLS update

$$\theta(k) = \theta(k{-}1) - P(k{-}1)\tilde{\Phi}(k)^{\rm T}\Gamma(k)^{-1}[\tilde{\Phi}(k)\theta(k{-}1) + \tilde{z}(k)],$$

where $P(k)$ satisfies

$$P(k) = P(k{-}1) - P(k{-}1)\tilde{\Phi}(k)^{\rm T}\Gamma(k)^{-1}\tilde{\Phi}(k)P(k{-}1),$$

$$\tilde{\Phi}(k) \triangleq \begin{bmatrix} \Phi_{\rm f}(k) \\ \Phi(k) \end{bmatrix} \in \mathbb{R}^{(l_y+l_d)\times l_\theta},$$

$$\tilde{R}(k) \triangleq \begin{bmatrix} R_z(k) & 0 \\ 0 & R_d(k) \end{bmatrix} \in \mathbb{R}^{(l_y+l_d)\times(l_y+l_d)},$$

$$\tilde{z}(k) \triangleq \begin{bmatrix} z(k) - \hat{d}_{\rm f}(k{-}1) \\ 0 \end{bmatrix} \in \mathbb{R}^{l_y+l_d},$$

$$\Gamma(k) \triangleq \tilde{R}(k)^{-1} + \tilde{\Phi}(k)P(k{-}1)\tilde{\Phi}(k)^{\rm T}.$$

B. State Estimation

In order to estimate the state $x(k)$, we modify the forecast step of the Kalman filter by including the input estimate $\hat{d}(k)$ as

$$x_{\rm f}(k) = Ax_{\rm da}(k-1) + G\hat{d}(k-1) + Bu(k-1), \tag{25}$$

$$P_{\rm f}(k) = AP_{\rm da}(k-1)A^{\rm T} + V_1, \tag{26}$$

where $x_{\rm f}(k) \in \mathbb{R}^{l_x}$ is the forecast state, $x_{\rm da}(k) \in \mathbb{R}^{l_x}$ is the data assimilation state, $P_{\rm f}(k) \in \mathbb{R}^{l_x\times l_x}$ is the forecast error covariance, and $P_{\rm da}(k) \in \mathbb{R}^{l_x\times l_x}$ is the data assimilation error covariance. The data assimilation step is given by

$$K_{\rm da}(k) = P_{\rm f}(k)C^{\rm T}S_{\rm da}^{-1}(k), \tag{27}$$

$$P_{\rm da}(k) = P_{\rm f}(k) - P_{\rm f}(k)C^{\rm T}S_{\rm da}^{-1}(k)CP_{\rm f}(k), \tag{28}$$

$$x_{\rm da}(k) = x_{\rm f}(k) + K_{\rm da}(k)\left[y(k) - Cx_{\rm f}(k)\right], \tag{29}$$

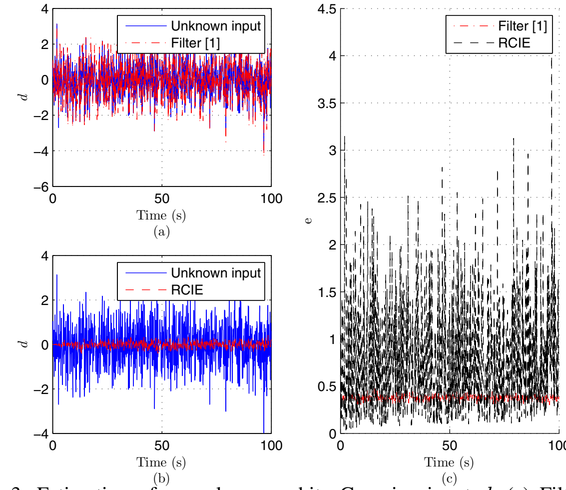

Fig. 3: Estimation of an unknown white Gaussian input d. (a) Filter [1] estimate. (b) RCIE estimate. (c) Error in the input estimate. The error for filter [1] (mean 0.37, standard deviation 0.04) is less than the error for RCIE (mean 0.83, standard deviation 0.58).

where $K_{\rm da}(k) \in \mathbb{R}^{l_x\times l_y}$ is the state estimator gain and $S_{\rm da}(k) \triangleq C(k)P_{\rm f}(k)C^{\rm T}(k) + V_2(k)$. Note that, if $\hat{d}(k) = d(k)$, then the state estimate is optimal in the sense of the standard Kalman filter.

III. Minimum-Phase Numerical Examples

We now apply *retrospective cost input estimation* (RCIE) to linear discrete-time MP systems, and compare it with filter [1]. Furthermore to assess the accuracy of the input estimate, we use the error metric

$$e(k) \triangleq \frac{1}{N_{\rm trial}}\sqrt{\sum_{i=1}^{N_{\rm trial}}\left[\hat{d}(k) - d(k)\right]^2}, \tag{30}$$

where $N_{\rm trial}$ is the number of trials, and plot (30) for RCIE and filter [1].

A. Highly Damped Plant

We consider Example 2 of [6]

$$A = \begin{bmatrix} 0.67 & 0 \\ 0 & 0.53 \end{bmatrix}, G = \begin{bmatrix} 1,00 \\ 0.53 \end{bmatrix}, C = \begin{bmatrix} 0.95 & 0,01 \\ 0.03 & 1.39 \end{bmatrix},$$

$$D_1 = D_2 = \begin{bmatrix} \sqrt{0.08} & 0 \\ 0 & \sqrt{0.08} \end{bmatrix}.$$

The system (A, G, C) has no transmission zeros. We set $\hat{x}(0) = x_{\rm da}(0) = [0\ 0]^{\rm T}$ and choose $N_{\rm trial} = 100, k_0 = 1, n_{\rm c} = 8, n_{\rm f} = 6, R_\theta = 500I_{l_\theta}, R_d = 0$, and $R_z = I_{l_y}$.

First, we let the unknown input d be white Gaussian noise with zero mean and unit variance as in [6]. Fig. 3 shows that the error for filter [1] (mean 0.37, standard deviation 0.03) is less than RCIE (mean 0.79, standard deviation 0.57). Next, we consider a case where the unknown input $d(k) = 1.5\left[\sin(kT_s) + \sin(2kT_s) + 1\right]$, that is, d is harmonic with two frequencies and a DC component. Fig. 4 shows that, after the initial transient, the error for RCIE (mean 0.45, standard deviation 0.31) converges close to the error for the filter [1] (mean 0.45, standard deviation 0.31).

B. Lightly Damped Plant

We now consider the mass-spring-damper system with two masses m_1, m_2, and an input force d on m_1. The dynamics are given by

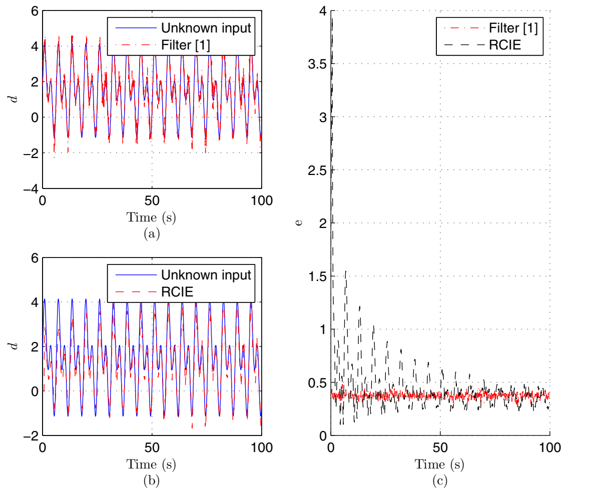

Fig. 4: Estimation of an unknown harmonic input d. (a) Filter [1] estimate. (b) RCIE estimate. (c) Error in the input estimate. After the initial transient, the error for RCIE (mean 0.45, standard deviation 0.31) converges close to the error for the filter [1] (mean 0.45, standard deviation 0.31).

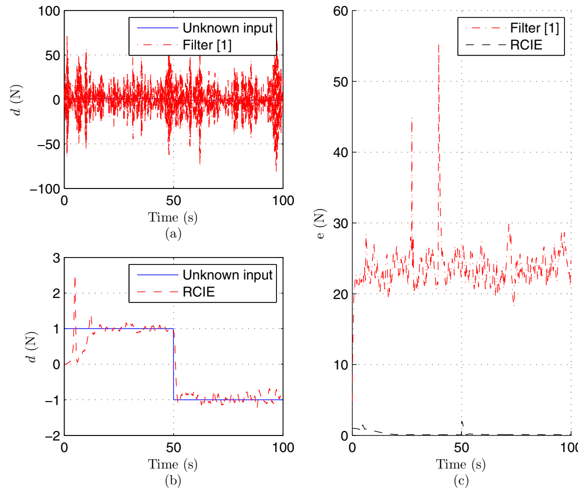

Fig. 5: Estimation of an unknown constant input for the lightly damped mass-spring-damper system. (a) Filter [1] estimate. (b) RCIE estimate. (c) Error in the input estimate. The error for RCIE is close to zero, whereas the error for filter [1] has mean 23.6 N and standard deviation 3.2 N.

$$\dot{x} = A_{\rm c}x + G_{\rm c}d, \tag{31}$$

where

$$A_{\rm c} \triangleq \begin{bmatrix} 0_{2\times 2} & I_{2\times 2} \\ \Omega_1 & \Omega_2 \end{bmatrix}, G_{\rm c} \triangleq \begin{bmatrix} 0_{2\times 1} \\ \Omega_3 \end{bmatrix}, \Omega_1 \triangleq \begin{bmatrix} -\frac{k_1+k_2}{m_1} & \frac{k_2}{m_1} \\ \frac{k_2}{m_2} & -\frac{k_2}{m_2} \end{bmatrix},$$

$$\Omega_2 \triangleq \begin{bmatrix} -\frac{c_1+c_2}{m_1} & \frac{c_2}{m_1} \\ \frac{c_2}{m_2} & -\frac{c_2}{m_2} \end{bmatrix}, \Omega_3 \triangleq \begin{bmatrix} \frac{1}{m_1} \\ 0 \end{bmatrix},$$

x_1 and x_2 are the displacements (m), and x_3 and x_4 are the velocities (m/s) of masses m_1 and m_2, respectively. We choose $m_1 = m_2 = 1\,\text{kg}, k_1 = k_2 = 1\,\text{N/m}$, and $c_1 = c_2 = 1\,\text{kg/s}$. We discretize (31) as

$$A = e^{A_{\rm c}T_{\rm s}}, \quad G = A_{\rm c}^{-1}(A_{\rm c} - I)G_{\rm c}, \tag{32}$$

where $T_{\rm s} = 0.1\,\text{s}$ is the sampling time. The discretized system has poles at $0.87 \pm 0.08\jmath$ and $0.97 \pm 0.05\jmath$. Letting

$$C = \begin{bmatrix} 1 & 0 & 0 & 0 \\ 0 & 1 & 0 & 0 \end{bmatrix},$$

we measure the mass positions and estimate the mass velocities and the unknown input force d on m_1. The system (A, G, C) has no transmission zeros. We set $\hat{x}(0) = x_{\rm da}(0) = [0\ 0\ 0\ 0]^{\rm T}$, $D_1 = 10^{-2}\text{diag}(1, 1, 2, 2)$, and $D_2 = 10^{-2}\text{diag}(1, 1)$. We choose $N_{\rm trial} = 100, k_0 = 0, n_{\rm c} = 4, n_{\rm f} = 4, R_\theta = 10^{-2}I_{l_\theta}, R_d = 10^{-8}$, and $R_z = I_{l_y}$.

We consider the case where the unknown input force d is constant. Fig. 5 shows that the error for RCIE is close to zero, whereas the error for filter [1] has mean 23.6 N and standard deviation 3.2 N.

IV. Nonminimum-Phase Numerical Examples

A. Mass-spring system

We reconsider the system (31) but with zero damping, that is, $c_1 = c_2 = 0$. Hence (31) is Lyapunov stable but not asymptotically stable. The continuous-time system has no transmission zeros, but the discretized system (A, G, C) has one transmission zero at -1 due to the sampling.

We consider the case where the unknown input force d is constant. Fig. 6 shows that the error for RCIE is 0.1 N at

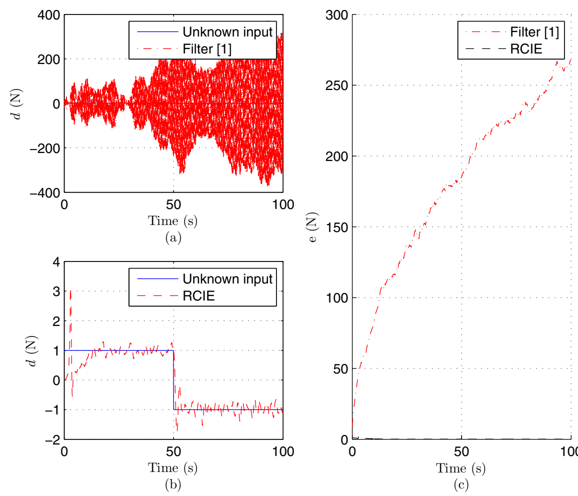

Fig. 6: Estimation of an unknown constant input for the undamped mass-spring system. (a) Filter [1] estimate. (b) RCIE estimate. (c) Error in the input estimate. The error for RCIE is close to zero, whereas the error for filter [1] keeps increasing.

$t = 100\,\text{s}$, whereas the error for the filter [1] keeps increasing and is 267.8 N at $t = 100\,\text{s}$.

Note that the filter [10] reduces to the filter [1] for the case where the measurement y does not depend on the unknown input d, which is the case considered in this paper. The behavior of the error shown in Fig. 6c with filter [1] for the NMP system is consistent with the stability condition (Theorem 6) given in [10].

B. Lateral Aircraft Dynamics Model

We consider the discretized lateral aircraft model [18]

$$A = \begin{bmatrix} 0.8482 & 0.0255 & -0.0900 & 0.0038 \\ -10.3212 & 0.8595 & 0.5152 & -0.0210 \\ 0.0186 & 0.0041 & 0.9723 & 0.0001 \\ -0.5304 & 0.0953 & -0.0239 & 0.9999 \end{bmatrix},$$

$$G = \begin{bmatrix} 0.0036 & 0.2390 & -0.0061 & 0.0124 \end{bmatrix}^{\rm T},$$

where $T_s = 0.1$ s, control input is the elevon deflection (rad) and $x = \begin{bmatrix} \beta & P & R & \phi_{\rm roll} \end{bmatrix}^{\rm T}$, that is, sideslip angle

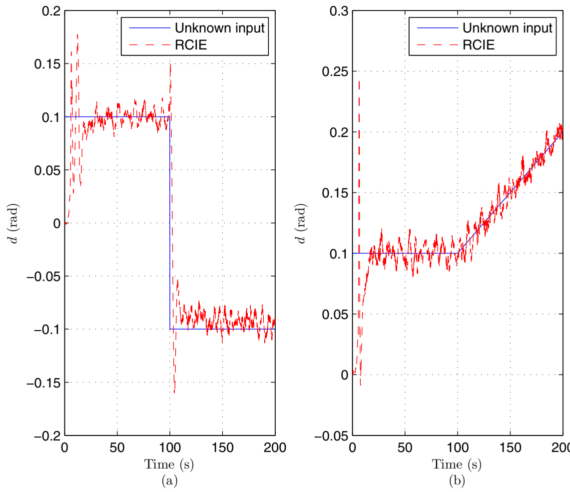

Fig. 7: Estimation of an unknown elevon deflection for the aircraft lateral dynamics. (a) Step deflection. (b) Ramp deflection. After the initial transient, RCIE estimates both the unknown step and ramp elevon deflection.

(rad), roll rate (rad/s), yaw rate (rad/s), and roll angle (rad). The roll-angle-to-elevon-deflection transfer function has two NMP zeros at -1.004 and 1.136. Letting $C = [0\,0\,0\,1]$, we measure roll angle and estimate elevon deflection. We set $\hat{x}(0) = x_{\rm da}(0) = [0\ 0\ 0\ 0]^{\rm T}$, $D_1 = 10^{-4}\ {\rm diag}(1,1,1,1)$, and $D_2 = 10^{-3}$. We choose $k_0 = 0, n_{\rm c} = 6, n_{\rm f} = 12, R_\theta = 10^{-4} I_{l_\theta}, R_d = 0$, and $R_z = 1$.

We consider two cases for estimating the unknown elevon deflection, namely, step deflection with height ± 0.1 rad, and ramp deflection with slope 0.001 rad/s. Fig. 7 shows that, after the initial transient, RCIE estimates both the unknown step and ramp elevon deflection of the aircraft. For comparison, the estimates of d using filters [1] and [10] diverges in less than 10 steps (not shown).

V. Experimental Results

A. Theoretical framework and experimental setup

The Earth and body-fixed frames are denoted by $\rm F_E$ and $\rm F_B$, respectively. We assume that $\rm F_E$ is an inertial frame and the Earth is flat. The origin $\rm O_E$ of $\rm F_E$ is any convenient point fixed on the Earth. The axes $\hat{\imath}_{\rm E}$ and $\hat{\jmath}_{\rm E}$ are horizontal, while the axis $\hat{k}_{\rm E}$ points downward. $\rm F_B$ is defined with $\hat{\imath}_{\rm B}$, $\hat{\jmath}_{\rm B}$ and $\hat{k}_{\rm B}$ fixed relative to the body. $\rm F_B$ and $\rm F_E$ are related by

$$\rm F_B = \vec{R}_{B/E}\, F_E, \tag{33}$$

where $\vec{R}_{\rm B/E}$ is a physical rotation matrix represented by a 3-2-1 Euler rotation sequence, involving two intermediate frames $\rm F_{E'}$ and $\rm F_{E''}$. In particular,

$$\vec{R}_{\rm B/E} = \vec{R}_{\hat{\imath}_{\rm E''}}(\Phi)\, \vec{R}_{\hat{\jmath}_{\rm E'}}(\Theta)\, \vec{R}_{\hat{k}_{\rm E}}(\Psi), \tag{34}$$

where $\rm F_{E'} = \vec{R}_{E'/E}\ F_E$, $\rm F_{E''} = \vec{R}_{E''/E'}\ F_{E'}$, and $\vec{R}_{\hat{n}}(\kappa)$ is the Rodrigues rotation about the eigenaxis $\hat{n}$ through the eigenangle κ according to the right-hand rule.

Let p denote a point that is fixed on the body. The location of p relative to $\rm O_E$ is denoted by $\vec{r}_{\rm p/O_E}$ and is resolved in $\rm F_E$ as

$$[X\quad Y\quad Z]^{\rm T} \triangleq \vec{r}_{\rm p/O_E}\Big|_{\rm E}. \tag{35}$$

The velocity of p relative to $\rm O_E$ with respect to $\rm F_E$ is

$$\vec{v}_{\rm p/O_E/E} = \overset{\rm E\bullet}{\vec{r}}_{\rm p/O_E}, \tag{36}$$

where E• denotes the derivative with respect to the time taken in Earth frame. The acceleration of p relative to $\rm O_E$ with respect to $\rm F_E$ is given by

$$\vec{a}_{\rm p/O_E/E} = \overset{\rm E\bullet}{\vec{v}}_{\rm p/O_E/E} = \overset{\rm E\bullet\bullet}{\vec{r}}_{\rm p/O_E}. \tag{37}$$

We resolve $\vec{a}_{\rm p/O_E/E}$ in $\rm F_E$ and $\rm F_B$ using the notation

$$\begin{bmatrix} A_x \\ A_y \\ A_z \end{bmatrix} \triangleq \vec{a}_{\rm p/O_E/E}\Big|_{\rm E}, \quad \begin{bmatrix} a_x \\ a_y \\ a_z \end{bmatrix} \triangleq \vec{a}_{\rm p/O_E/E}\Big|_{\rm B}. \tag{38}$$

Using (34) and (38), $\vec{a}_{\rm p/O_E/E}$ in $\rm F_E$ is given by

$$\vec{a}_{\rm p/O_E/E}\Big|_{\rm E} = \mathcal{O}_{\rm E/B}\, \vec{a}_{\rm p/O_E/E}\Big|_{\rm B}, \tag{39}$$

and thus,

$$\begin{bmatrix} A_x & A_y & A_z \end{bmatrix}^{\rm T} = \mathcal{O}_{\rm E/B} \begin{bmatrix} a_x & a_y & a_z \end{bmatrix}^{\rm T}, \tag{40}$$

where

$$\mathcal{O}_{\rm E/B} = \vec{R}_{\rm E/B}\Big|_{\rm E}.$$

Note that (33)–(40) are kinematic relations that are applicable to an arbitrary point p on a body and are independent of all modeling information.

For estimating the inertial acceleration of p relative to $\rm O_E$ with respect to $\rm F_E$, (36)–(40) are written in state space form

$$\dot{x} = A_{\rm c} x + G_{\rm c} d, \tag{41}$$

where

$$A_{\rm c} = \begin{bmatrix} 0_{3\times3} & I_{3\times3} \\ 0_{3\times3} & 0_{3\times3} \end{bmatrix}, \quad G_{\rm c} = \begin{bmatrix} 0_{3\times3} \\ I_{3\times3} \end{bmatrix},$$

$$x = \begin{bmatrix} X & Y & Z & \dot{X} & \dot{Y} & \dot{Z} \end{bmatrix}^{\rm T}, d = \begin{bmatrix} A_x & A_y & A_z \end{bmatrix}^{\rm T},$$

whereas, for estimating the inertial acceleration of p relative to $\rm O_E$ with respect to $\rm F_B$, (36)–(40) are written as

$$\dot{x} = A_{\rm c} x + G_{\rm c} d, \tag{42}$$

where

$$A_{\rm c} = \begin{bmatrix} 0_{3\times3} & I_{3\times3} \\ 0_{3\times3} & 0_{3\times3} \end{bmatrix}, \quad G_{\rm c} = \begin{bmatrix} 0_{3\times3} \\ \mathcal{O}_{\rm E/B} \end{bmatrix},$$

$$x = \begin{bmatrix} X & Y & Z & \dot{X} & \dot{Y} & \dot{Z} \end{bmatrix}^{\rm T}, d = \begin{bmatrix} a_x & a_y & a_z \end{bmatrix}^{\rm T}.$$

Note that (41) and (42) are exact kinematic equations, and thus do not include sensor noise. The source of process noise in (42) is noisy measurements of Φ, Θ, and Ψ, which are used to compute $\mathcal{O}_{\rm E/B}$.

In the laboratory setup, we estimate the inertial acceleration of a quadrotor in $\rm F_E$ and $\rm F_B$ using (41) and (42), respectively, with $C = \begin{bmatrix} I_{3\times3} & 0_{3\times3} \end{bmatrix}$. The position $\vec{r}_{\rm p/O_E}\Big|_{\rm E}$ and attitude (Φ, Θ, Ψ) of the vehicle are obtained using the Vicon system and recorded for post-flight data analysis. To compare the estimated acceleration with the measured acceleration, data from the vehicle's inertial measurement unit (IMU) is recorded and time-stamped. Using knowledge of the vehicle attitude, IMU acceleration measurements are corrected to compensate for gravity offset for comparison with RCIE acceleration estimates.

B. Estimating inertial acceleration in the Earth frame

We discretize (41) using (32) with $T_{\rm s}$=0.01 s, which is the sample-rate of the recorded data. The system (A, G, C) is NMP with six poles at 1 and three transmission zeros at -1. We set $D_1 = 10^{-1} I_{6\times6}$, and $D_2 = 10^{-1} I_{3\times3}$, and choose k_0=0, $n_{\rm c}$=12, $n_{\rm f}$=6, R_θ=$10^{-6} I_{l_\theta}$, R_d=$10^{-4} I_{l_d}$, R_z=I_{l_y}.

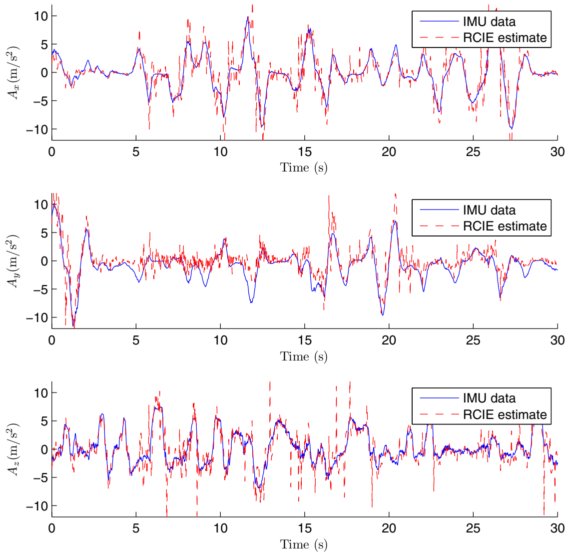

Fig. 8: Estimation of the inertial acceleration of the quadrotor relative to $\mathrm{O_E}$ with respect to $\mathrm{F_E}$ using position measurements. RCIE estimates are compared with the IMU acceleration measurements transformed to $\mathrm{F_E}$ and corrected to compensate for gravity offset.

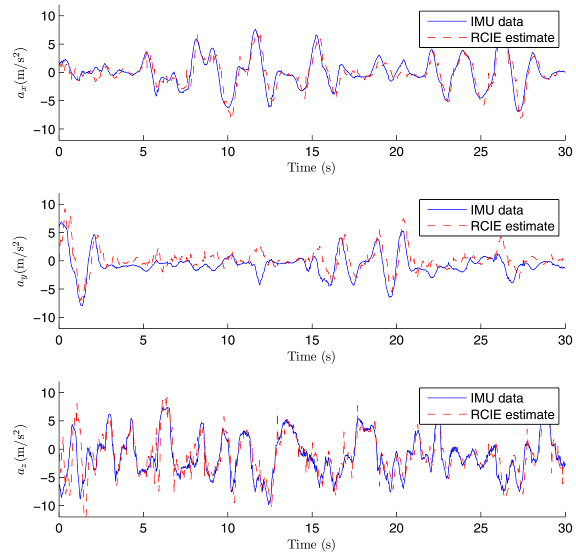

Fig. 9: Estimation of the inertial acceleration of the quadrotor relative to $\mathrm{O_E}$ with respect to $\mathrm{F_B}$ using position and attitude measurements. RCIE estimates are compared with the IMU acceleration measurements with gravity correction.

Fig. 8 shows the accuracy of the RCIE estimate of the inertial acceleration of the quadrotor in $\mathrm{F_E}$ using position measurements obtained from the Vicon system. For this setup, the estimates of d using filters [1] and [10] diverge in less than 250 steps (not shown).

C. Estimating inertial acceleration in the body frame

Noting that G_{c} is time varying in (42), we discretize (42) at each time step k using (32) with $T_{\mathrm{s}} = 0.01\,\mathrm{s}$, which is the sample-rate of the recorded data. We choose $D_1 = 10^{-2} I_{6\times 6}$, and $D_2 = 10^{-1} I_{3\times 3}$, $k_0 = 0, n_{\mathrm{c}} = 12, n_{\mathrm{f}} = 6, R_\theta = 10^{-10} I_{l_\theta}, R_d = 10^{-4} I_{l_d}$, and $R_z = I_{l_y}$.

Fig. 9 shows the accuracy of the RCIE estimate of the inertial acceleration of the quadrotor in the body frame using position and attitude measurements obtained from the Vicon system. For this setup, the estimates of d using filters [1] and [10] diverge in less than 250 steps (not shown).

VI. Conclusion

This paper presented an extension of retrospective cost input estimation (RCIE) and demonstrated its applicability to nonminimum-phase systems. Input estimation was performed for both numerical examples and for laboratory data, where camera measurements were used to estimate acceleration with validation based on onboard accelerometers.

VII. Acknowledgment

We wish to thank Dimitra Panagou and Wei Ding for providing the Vicon and quadrotor data used in this paper. This research was supported in part by the Office of Naval Research under grant N00014-14-1-0596.

References

[1] S. Gillijns and B. De Moor, "Unbiased minimum-variance input and state estimation for linear discrete-time systems," *Automatica*, pp. 111–116, 2007.

[2] C.-S. Hsieh, "Extension of unbiased minimum-variance input and state estimation for systems with unknown inputs," *Automatica*, pp. 2149–2153, 2009.

[3] H. Khaloozadeh and A. Karsaz, "Modified input estimation technique for tracking manoeuvring targets," *Radar, Sonar & Navigation, IET*, pp. 30–41, 2009.

[4] R. Orjuela, B. Marx, J. Ragot, and D. Maquin, "On the simultaneous state and unknown input estimation of complex systems via a multiple model strategy," *Contr. Theory & Applic.*, pp. 877–890, 2009.

[5] M.-S. Chen and C.-C. Chen, "Unknown input observer for linear non-minimum phase systems," *J. Franklin Institute*, pp. 577–588, 2010.

[6] H. Fang, Y. Shi, and J. Yi, "On stable simultaneous input and state estimation for discrete-time linear systems," *I. J. Adap. Contr. Sig. Proc.*, pp. 671–686, 2011.

[7] J. Yang, F. Zhu, and X. Sun, "State estimation and simultaneous unknown input and measurement noise reconstruction based on associated observers," *I. J. Adap. Contr. Sig. Proc.*, pp. 846–858, 2013.

[8] A. Termehchy and A. Afshar, "A novel design of unknown input observer for fault diagnosis in non-minimum phase systems," in *World Congress*, 2014, pp. 8552–8557.

[9] J. Sanchez and H. Benaroya, "Review of force reconstruction techniques," *J. Sound Vibration*, no. 14, pp. 2999–3018, 2014.

[10] S. Z. Yong, M. Zhu, and E. Frazzoli, "A unified filter for simultaneous input and state estimation of linear discrete-time stochastic systems," *Automatica*, pp. 321–329, 2016.

[11] P. K. Kitanidis, "Unbiased minimum-variance linear state estimation," *Automatica*, pp. 775–778, 1987.

[12] M. Darouach and M. Zasadzinski, "Unbiased minimum variance estimation for systems with unknown exogenous inputs," *Automatica*, pp. 717–719, 1997.

[13] A. M. D'Amato and D. S. Bernstein, "Adaptive forward-propagating input reconstruction for nonminimum-phase systems," *Proc. Amer. Conf. Contr.*, pp. 598–603, Montreal, 2012.

[14] R. Gupta, A. M. D'Amato, A. A. Ali, and D. S. Bernstein, "Retrospective-cost-based adaptive state estimation and input reconstruction for a maneuvering aircraft with unknown acceleration," in *AIAA Guid. Nav. Contr. Conf.*, 2012, p. 4600.

[15] A. A. Ali, A. Goel, A. J. Ridley, and D. S. Bernstein, "Retrospective-cost-based adaptive input and state estimation for the ionosphere–thermosphere," *J. Aerospace Information Systems*, pp. 1–17, 2015.

[16] L. Han, A. Xie, Z. Ren, and D. S. Bernstein, "Maneuvering target tracking with unknown acceleration using retrospective-cost-based adaptive input and state estimation," in *Proc. 34th Chinese Contr. Conf.*, 2015, pp. 5029–5034.

[17] A. Ansari and D. S. Bernstein, "Aircraft sensor fault detection using state and input estimation," *Proc. Amer. Contr. Conf.*, Boston, 2016.

[18] A. Ansari and D. S. Bernstein, "Adaptive Control of an Aircraft with Uncertain Nonminimum-Phase Dynamics," *Proc. Amer. Contr. Conf.*, pp. 844–849, Chicago, 2015.